Hydration and Dewetting near Graphite−CH_3 and Graphite−COOH Plates

Jingyuan Li,[†,‡] Ting Liu,[§] Xin Li,[||] Lei Ye,[§] Huajun Chen,[§] Haiping Fang,[‡] Zhaohui Wu,[§] and Ruhong Zhou*[,||,⊥]

Department of Physics, Zhejiang University, Hangzhou 310027, China, Shanghai Institute of Applied Physics, Chinese Academy of Science, Shanghai 201800, China, Department of Computer Science, Zhejiang University, Hangzhou 310027, China, Department of Chemistry, Columbia University, New York, New York 10027, and IBM Thomas J. Watson Research Center, Yorktown Heights, New York 10598

Received: December 28, 2004; In Final Form: April 21, 2005

The dynamics of water near the nanoscale hydrophobic (graphite−CH_3) and hydrophilic (graphite−COOH) plates has been studied in detail with molecular dynamics simulations in this paper. It is shown that these designed surfaces (by growing a layer of methyl or carboxyl groups on top of graphite) can have a significant impact on the neighboring water dynamics, with the hydrophilic carboxyl surface having even more profound effects. The water hydrogen bond lifetime is much longer near both types of surfaces than that in the bulk, while on the other hand the water diffusion constant is much smaller than that in the bulk. The difference in the diffusion constant can be as large as a factor of 8 and the difference in the hydrogen bond lifetime can be as large as a factor of 2, depending on the distance from the surface. Furthermore, the water molecules in the first solvation shell of surface atoms show a strong bias in hydroxyl group orientation near the surface, confirming some of the previous findings. Finally, the possible water dewetting transition between two graphite−CH_3 plates and the effect of the strength of the solute−solvent attractions on the water drying transition are investigated. The relationship among the dewetting transition critical distance, van der Waals potential well depth, and water contact angle on the graphite−CH_3 surface is also analyzed on the basis of a simple macroscopic theory, which can be used to predict the dewetting transition critical distance.

1. Introduction

The complex nature of the interface between water and hydrophobic surfaces has long been recognized as the key for understanding the hydrophobic effect, which plays an important role in many fields such as protein folding,[1−4] self-assembly of amphiphiles,[5] water permeation in membrane channels or pores (aquaporins),[6,7] and capillary evaporation.[8−10] Many biomolecules, such as proteins, are characterized by surfaces containing extended nonpolar hydrophobic and polar hydrophilic regions. The aggregation and subsequent removal of water molecules among hydrophobic surfaces are believed to be critical for the folding, structure, and function of proteins. Unfortunately, the complicated nature of protein folding and protein−water interactions often make it a highly nontrivial practice to directly probe the hydrophobic effect in these complicated systems.[11−13] On the other hand, much can be learned by studying a similar but structurally less complicated problem, such as the hydration and collapse of graphite−CH_3 and graphite−COOH plates, constructed by growing a layer of methyl (−CH_3) or carboxyl (−COOH) groups on top of a graphite sheet.

It is now widely believed that the mechanism of hydration of small hydrophobic solutes is different from that of large ones. Small solutes such as methane can fit into the water hydrogen bond network without significantly perturbing the water hydrogen bonds,[14] whereas larger hydrophobic solutes tend to break the water hydrogen bond network and force the reorganization of water molecules.[15,16] Simulations have also shown that the surfaces of large solutes can have a significant impact on the hydration and water dynamics near the interface.[11,17−21] For example, Cheng and Rossky have found that certain hydrophobic residues on protein mellitin do not break neighboring water hydrogen bonds, whereas other residues do, leading to a heterogeneous distribution of hydrophobic surfaces.[11] Sansom and co-workers have observed a liquid−vapor oscillation of water in a hydrophobic nanopore when studying the hydrophobic gating mechanism for membrane pores (aquaporins).[6,7] More interestingly, a dewetting layer filled with as many as several water molecules around strongly hydrophobic surfaces might exist, as first suggested by Stillinger.[22] This vapor layer is also predicted by modern density functional theories such as the Lum−Chandler−Weeks (LCW) theory.[23,24] The Chandler group has studied the water dewetting near hydrophobic solutes extensively, using a combination of analytical theories and coarse-grained model simulations.[23−27] Early studies by Wallqvist and Berne have also indicated that when two strongly hydrophobic plates (Gay−Berne ellipsoids) are brought together, the water is expelled from the interplate region even though there is enough space for more than one layer of water.[28] The spontaneous dewetting provides a very strong driving force for hydrophobic collapse. Some other groups have addressed related issues with simpler solutes as well.[5,10,29−34] However, although much has been learned about the hydrophobic effect from these studies on simple solutes, the hydrophobic interactions in macromolecules, such as those in protein folding, remain largely unknown. By comparison, much less work has been done on

* To whom correspondence should be addressed. E-mail: ruhongz@us.ibm.com.
[†] Department of Physics, Zhejiang University.
[‡] Chinese Academy of Science.
[§] Department of Computer Science, Zhejiang University.
[||] Columbia University.
[⊥] IBM Thomas J. Watson Research Center.

10.1021/jp044090w CCC: $30.25
Published on Web 06/25/2005

these systems. Such difficulty is partly due to the lack of amenable systems for study.

In this work, we devise a model system of moderate structural complexity which is readily manageable yet without losing the essence of the underlying physical picture. More specifically, we artificially grow a layer of $-CH_3$ or $-COOH$ groups on top of a graphite layer. This will not only allow us to study the different water hydration behaviors near the hydrophobic (methyl groups) and hydrophilic (carboxyl groups) surfaces but also allow us to probe possible dewetting transitions between two such surfaces. Furthermore, we can easily mimic the protein "hydrophobic core" or "hydrophilic exterior" by manipulating the relative population of $-CH_3$ and $-COOH$ groups, given that not all residues in the protein hydrophobic core are hydrophobic and not all residues in the protein hydrophilic exterior are hydrophilic.

Interestingly, recent experimental evidence of the existence of the vapor layer of molecular size around polystyrene[35] and paraffin-like molecules[36,37] has also been reported.[38] The water density at the depletion layers is about 6−12%[35] and ∼10%[36] lower than the bulk water density near the polystyrene and paraffin surfaces, respectively. Very recently, Zhou and co-workers[13] have also looked at the hydrophobic collapse and possible dewetting in multidomain protein folding,[13] and weak water depletion with water density about 10−15% lower than the bulk has been found in the interdomain region. Furthermore, a strong dewetting transition can be observed if the attractive portions of the protein−water interactions are turned off, even though the protein domain interfaces are much more complicated than the "polished" paraffin surfaces.[13,36] This new evidence makes the comparative study of the hydration and dewetting of simplified systems, such as graphite−CH_3 and graphite−COOH plates, even more interesting and timely. To our knowledge, this is the first attempt to grow a layer of methyl and carboxyl groups on top of graphite to mimic the protein hydrophobic and hydrophilic surfaces in order to address the water hydration and dewetting problems.

This paper is organized as follows. The graphite−CH_3 and graphite−COOH model systems and computational methods are described in section 2. Section 3 gives detailed simulation results on the hydration and hydrophobic collapse of graphite−CH_3 and graphite−COOH plates as well as a comparison with our previous results from multidomain protein folding and paraffin-plate collapse. The last section provides the conclusion and remarks of future directions. The current work demonstrates that much can be learned from these newly designed but structurally less complex systems.

2. System and Methods

In the present study, a layer of methyl ($-CH_3$) or carboxyl ($-COOH$) groups on top of a graphite surface is designed to mimic the hydrophobic or hydrophilic surfaces. Each elementary cell of the graphite surface has dimensions of 4.2×2.42 Å^2. The graphite layer is constructed from 8×14 elementary cells, leading to a surface dimension of 33.6×29.0 Å^2. A total of 63 methyl or carboxyl groups with equal spacing are then anchored to the graphite surface (see Figure 1). The density of the active sites (the sites with a methyl or carboxyl group) is about 4.92 site/(100 Å^2), as the active groups are "planted" in every other elementary cell. Except for the C(graphite)−C(CH_3) and C(graphite)−C(COOH) bonds which are designed to be perpendicular to the graphite surface, the rest of the $-CH_3$ and $-COOH$ geometries follow the typical minimized force field geometries and are free to move during the simulation. Both a single surface (referred to as "single plate" in the following) and double surfaces with the methyl or carboxyl groups facing each other ("double plates") are studied in this work. The plates (either single or double) are then solvated in a $60 \times 60 \times 60$ Å^3 water box with a total of about 22 000 atoms.

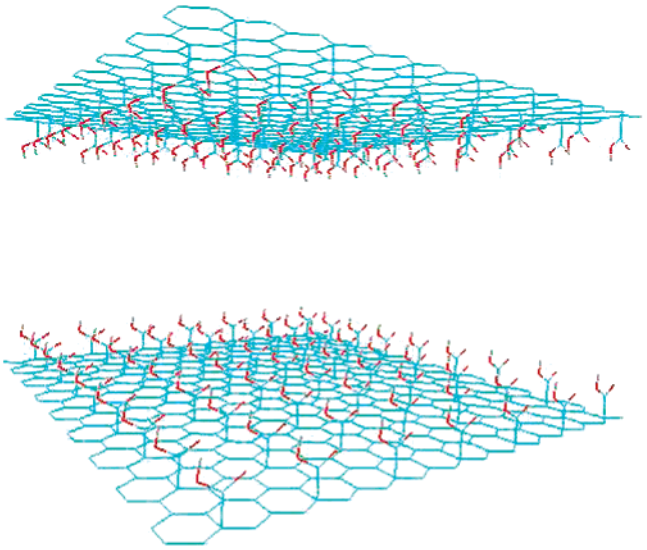

Figure 1. Scheme of the two graphite sheets planted with carboxyl groups. In this study, both single plates and double plates planted with methyl and carboxyl groups are used. These plates are then solvated in a $60 \times 60 \times 60$ Å^3 water box. The methyl and carboxyl groups are free to move during the simulation, even though they are initially set up to have identical orientations, as shown in the figure.

TABLE 1: Detailed Force Field Parameters Used for the Lennard-Jones Interactions ($V_{LJ}(r_{ij}) = 4\epsilon_{ij}[(\sigma_{ij}/r_{ij})^{12} - (\sigma_{ij}/r_{ij})^6]$) and Coulomb Interactions in the Graphite−COOH and Graphite−CH_3 Plates, Including the Carbon Atom in Graphite Plate and Atoms in Both the Methyl ($-CH_3$) and Carboxyl ($-COOH$) Groups

atom type	σ (Å)	ϵ (kcal/mol)	charge (e)
C (graphite)	3.55	0.070	0.000
C (COOH)	3.75	0.105	0.520
Oc (COOH)	2.96	0.210	−0.440
Oh (COOH)	3.00	0.170	−0.530
H (COOH)	0.00	0.00	0.450
C (CH_3)	3.50	0.066	−0.180
H (CH_3)	2.50	0.030	0.060

A modified GROMACS[39] program is used for the molecular dynamics simulations. Both constant pressure−constant temperature (NPT, 1 atm and 300 K) and constant total-energy (NVE) simulations are performed for data collection with a time step of 1.0 fs. A standard equilibration procedure, which includes a conjugate gradient minimization and a 100 ps position restrained molecular dynamics equilibration, is used to equilibrate the system. The final configurations after equilibration are then used for data collection. The OPLSAA force field[40] is used for the graphite sheet as well as the methyl and carboxyl groups (see Table 1 for the detailed parameters), and the SPC water model is used for the explicit solvent. The particle mesh Ewald (PME) method is adopted for the long-range electrostatic interactions, whereas a typical 10 Å cutoff is applied to the van der Waals interactions.

3. Results and Discussion

Water hydration near both the single and double graphite−CH_3 and graphite−COOH plates is studied in this work in order to understand the detailed water dynamics near the hydrophobic and hydrophilic surfaces. This includes the water hydrogen bond

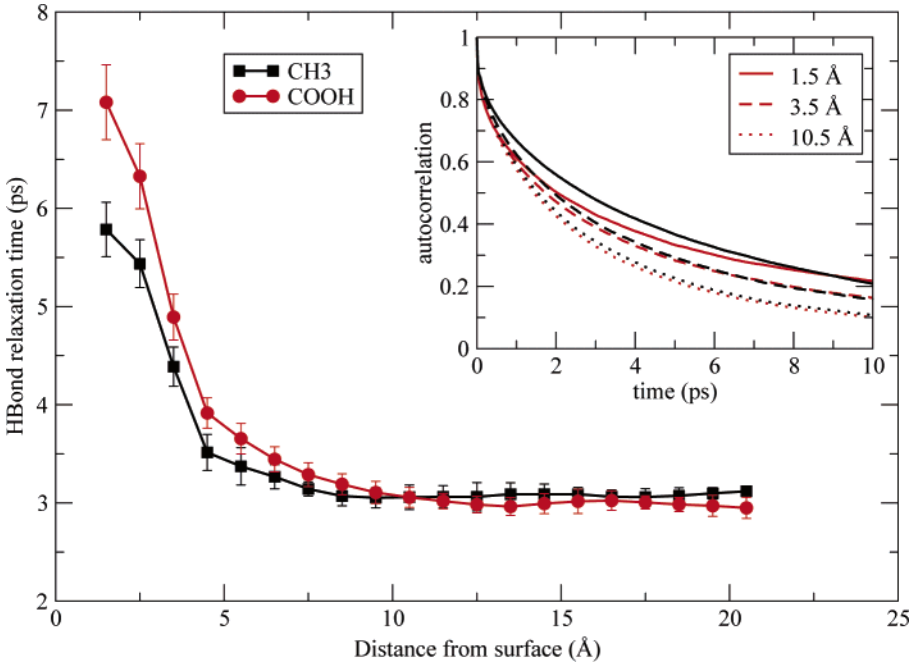

Figure 2. Water hydrogen bond relaxation time, τ, versus the distance from the surface (z-coordinate) for both the methyl (black) and carboxyl (red) surfaces. The data and error bars are computed from eight 200 ps NVE simulations. A water layer of 3 Å thick parallel to the surface is used for data averaging. The inset shows several examples of raw data for the water autocorrelation function, $C(t)$, at z = 1.5 Å (solid line), 3.5 Å (dashed line), and 10.5 Å (dotted line) for both the methyl (black) and carboxyl (red) surfaces.

relaxation lifetime, water self-diffusion constant, the first solvation shell hydroxyl group orientation, and the possible dewetting or water drying transitions between the double hydrophobic plates. For simplicity, the coordinate system is set up such that all the plates are perpendicular to the z-axis. The single plates are facing up (the active groups having larger z-coordinates than graphite atoms) with the z-coordinate of the highest active group atom set to zero (the $x-y$ origin is set to the center of the plate). The double plates are set up in a similar way with the lower plate the same as the single plate case and the upper plate facing down. For example, the interplate region for double plates with a plate−plate distance of 13 Å can be described as the region with $-16.8 < x < 16.8$ Å, $-14.5 < y < 14.5$ Å, and $0 < z < 13$ Å. The $x-y$ plane thus describes the water layers parallel to the plate surfaces. As will be seen in the following, most of the water properties will be described as a function of z. Also, each data point along the z-axis is averaged over a layer of 3.0 Å thick in order to have enough water molecules for averaging.

3.1. Water Dynamics near a Single Plate. It is expected that the water molecules near the surfaces might rotate slowly due to the hydrogen bonds to the hydrophilic surface or due to hydrophobic effects near the hydrophobic surfaces. It is interesting to know quantitatively how much of an effect the hydrophobic and hydrophilic surfaces can have on the water hydrogen bond relaxation time, which is characterized by the hydrogen bond autocorrelation function[41]

$$C(t) = \frac{\langle h(0)\, h(t)\rangle}{\langle h(0)\, h(0)\rangle} \qquad (1)$$

where $h(t) = 1$ if the tagged water pair is hydrogen bonded at time zero to time t and $h(t) = 0$ otherwise. We adopt a geometric definition of the hydrogen bond; namely, two water molecules are considered to be hydrogen bonded if their oxygen−oxygen distance is less than 3.5 Å, and the angle O−H···O is greater than 150° simultaneously.[17] Thus, $C(t)$ describes the probability of a pair of water molecules being hydrogen bonded at time $t = 0$ and still hydrogen bonded at time t.

Figure 2 shows the autocorrelation functions for both the $-CH_3$ and −COOH surfaces in the inset (black for $-CH_3$ and red for −COOH. The same color scheme is used throughout the paper). Results from three representative layers at z = 1.5, 3.5, and 10.5 Å for both methyl and carboxyl groups are shown. As expected, the autocorrelation function, $C(t)$, decays exponentially in both cases, with the decay constant revealing the hydrogen bond relaxation time. It is interesting to note that $C(t)$ becomes essentially the same for $-CH_3$ and −COOH surfaces at z = 10.5 Å, indicating that at this distance the hydrogen bond relaxation time becomes the same for both surfaces which essentially mimics the bulk.

The hydrogen bond lifetime, τ, is then obtained by fitting the autocorrelation function, $C(t)$, with the single exponential decay function $C(t) = Ae^{-t/\tau}$ at the time interval [0.3 ps, 15 ps]. As pointed out previously,[42,43] fitting the autocorrelation function can be nontrivial, since it does not decay perfectly as a single exponential. Others have tried a double exponential (using the longer τ_{long} as the lifetime), triple exponential (using the mid τ_{mid} as the lifetime), and stretched single exponential $C(t/\tau) = Ae^{-(t/\tau)^{\beta}}$ (Kohlrausch−William−Watts (KWW) fit[44,45] by setting $C(\tau) = e^{-1}$) for the hydrogen bond lifetime.[42,43] Here, we simplify the problem by choosing a time interval ([0.3 ps, 15 ps]) for fitting to avoid the sharp decay in the first tenths of a picosecond and slower decay after several lifetimes. We have also tried the double exponential and KWW fittings; the detailed lifetime values vary somewhat, but the trend does not change, which is really the main focus of this study here. The final results are shown in Figure 2. The average and error bar are computed from eight 200 ps NVE simulations starting from different initial configurations. These results show that both surfaces have a significant impact on the water hydrogen bond lifetime, with the impact from the carboxyl groups being even more dramatic. A much longer relaxation time is found for water molecules near the surfaces than those far away from the surfaces. The

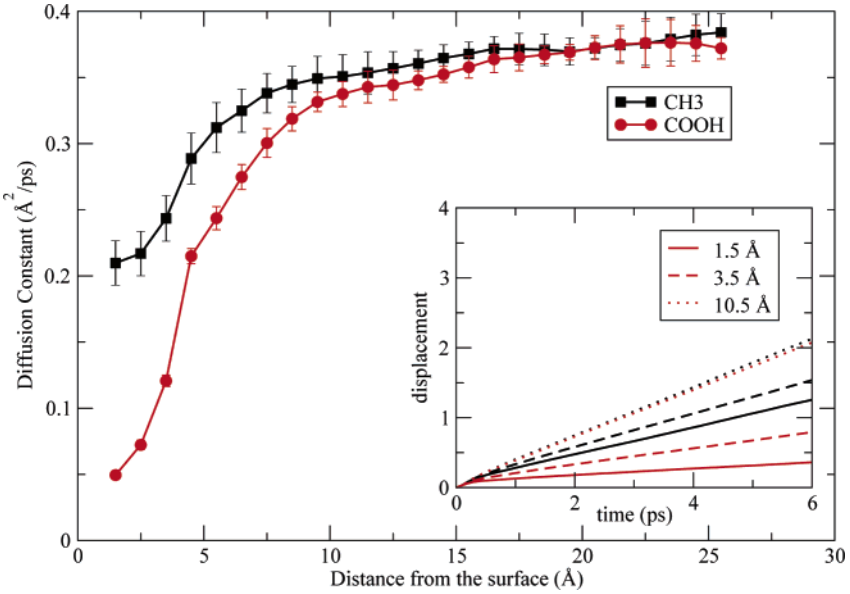

Figure 3. Water self-diffusion constant, D, versus the distance from the surface for both the methyl (black) and carboxyl (red) surfaces. The data and error bars are computed from eight 200 ps NVE simulations. A water layer of 3 Å thick parallel to the surface is used for data averaging. The inset shows several examples of raw data for the water mean square displacement at $z = 1.5$ Å (solid line), 3.5 Å (dashed line), and 10.5 Å (dotted line) for both the methyl (black) and carboxyl (red) surfaces.

longest relaxation time near the carboxyl surface is 7.08 ± 0.38 ps, which is more than twice the bulk value 2.98 ± 0.08 ps. The relaxation time near the methyl surface, 5.79 ± 0.28 ps, is also about twice the bulk value. These results clearly indicate that solute surfaces, either hydrophobic or hydrophilic, can significantly increase the hydrogen bond lifetime. Also, this lifetime increase can extend to fairly long distances from the surface, as large as 8−10 Å in this case, which is slightly larger than the 5−8 Å range previously found by other groups.[46,47] The following water diffusion constant results will show similar effects but with an even longer scale, up to 15 Å. Interestingly, a water molecule near the hydrophilic (−COOH) surface has about a 20% longer hydrogen bond lifetime than one near the hydrophobic (−CH_3) surface. The longer lifetime near the −COOH surface is mainly due to the strong hydrogen bonds between water molecules and the carboxyl groups, which enhance the stability of the water hydrogen bonds and attenuate the water mobility. The longer than bulk hydrogen bond lifetime for water molecules near the hydrophobic surface (−CH_3), on the other hand, is mainly due to the so-called hydrophobic effects. For a water molecule in the bulk, it can easily make a new hydrogen bond with neighboring water molecules when breaking an old one, which provides a "mediation" to lower the free energy barrier for breaking a hydrogen bond. However, for a water molecule near the hydrophobic methyl surface, such mediation is largely gone because no hydrogen bonds can be formed between water and these methyl groups. Thus, the free energy barrier for breaking a water hydrogen bond near the hydrophobic surface is higher than the bulk, which results in a longer hydrogen bond lifetime.

Another related aspect is the surface effect on the water mobility or self-diffusion constant. It is predicted that the water molecules should diffuse more slowly near the surfaces due to similar reasons to those described above for the longer hydrogen bond relaxation time. One good way to show this is to measure the mean square displacement of water as a function of the distance from the surface. The results are shown in the inset of Figure 3. Again, three representative layers are shown for both surfaces at $z = 1.5$, 3.5, and 10.5 Å, respectively. These data exhibit a clear linear relationship between the water mean square displacement and the time, t. In principle, one needs to solve the Smoluchowski equation,[48] as pointed out by Berne and coworkers,[46] to obtain diffusion constants for water molecules in a region with a nonzero potential of mean force, such as water−vapor interfaces, water−solute interfaces, or confined water.[46] It is nontrivial to calculate an accurate potential of mean force for the water molecules near the nonuniform various sites on the methyl or carboxyl plates. However, the above linear relationship between the mean square displacement and time t indicates that an estimate from the Einstein relation might be good enough for the diffusion constant, D_w. Thus, we follow previous studies[49,50] to use this simple approach for the diffusion constant.

$$D_w = \frac{\langle |r_i(t) - r_i(0)|^2 \rangle}{6t} \tag{2}$$

The results are shown in Figure 3. Clearly, the diffusion of water molecules is slowed dramatically by the carboxyl and methyl groups. The smallest diffusion constant near the −COOH surface is 0.049 ± 0.003 Å²/ps, which is about 8 times smaller than the bulk value 0.375 ± 0.016 Å²/ps. The water diffusion constant near the −CH_3 surface, 0.210 ± 0.017 Å²/ps, is also significantly lower than the bulk value. Again, these results indicate that solute surfaces can have a significant impact on the water mobility near the surface. Compared with the above hydrogen bond lifetime results, the surface effect on the water self-diffusion constant seems to be even more profound. Not only do the diffusion constants differ more than the bulk, by a factor of ∼8 in the −COOH case, but also the effect extends into greater distances from the surface, up to 15 Å in this case. As mentioned earlier, this is larger than the distances previously found by other groups.[46,47] The water diffusion constant near the hydrophilic (−COOH) surface is also ∼4 times smaller than that near the hydrophobic (−CH_3) surface. These results are generally consistent with the above hydrogen bond lifetime results. Both the methyl and carboxyl groups immobilize the water molecules around them. The influence of the surface is found up to 10−15 Å, with the carboxyl groups having more profound effects. It is such immobility due to either strong

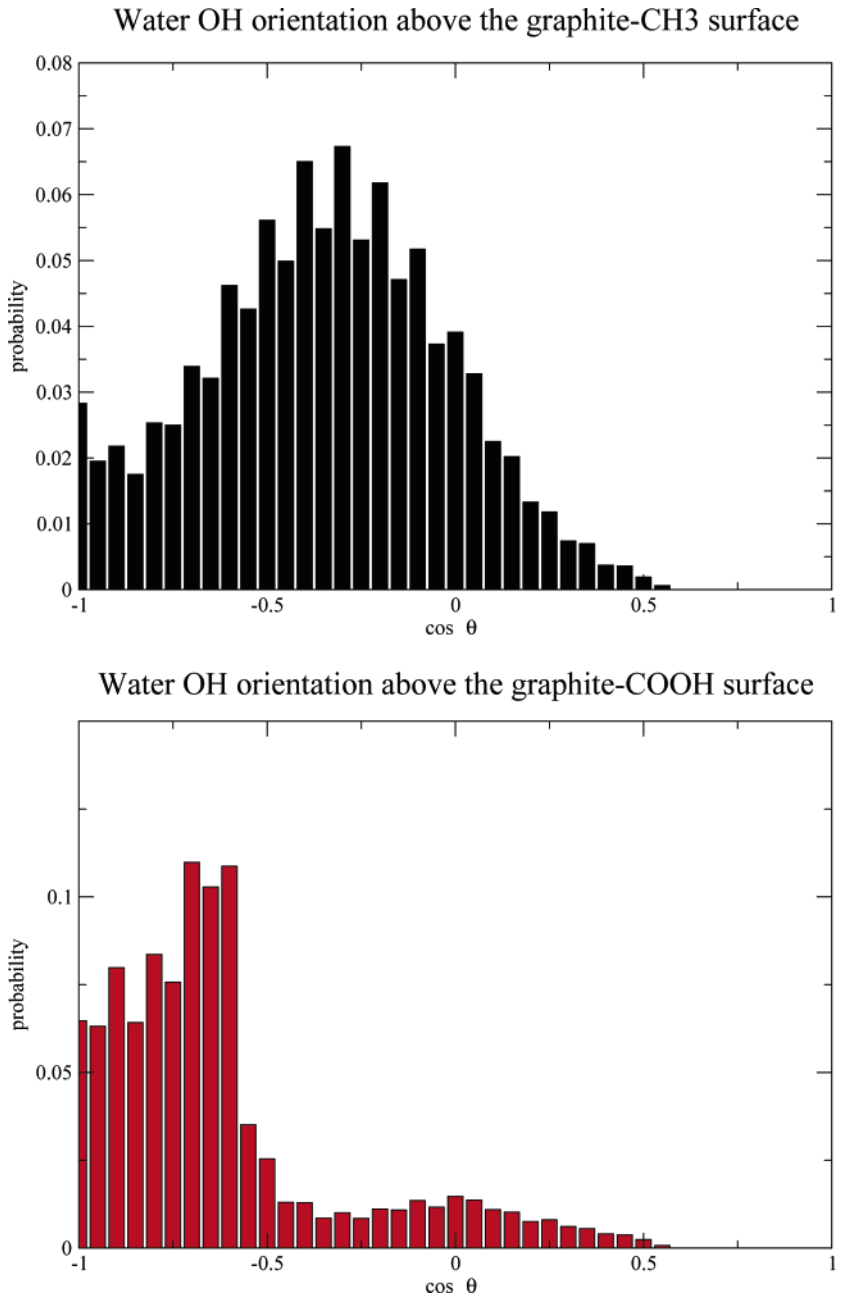

Figure 4. Distribution profile of cos(θ) for the angle, θ, between the first solvation shell water hydroxyl groups and the surface normal on both methyl (black) and carboxyl (red) surfaces. See the text for details of the angle definition. Both surfaces show a strong bias in the water hydroxyl group orientation by pointing the O−H vectors to the surface.

hydrogen bonds or hydrophobic effects that is responsible for both the enhancement of the hydrogen bond lifetime and the attenuation of the self-diffusion constant.

The first solvation shell of the hydrophobic or hydrophilic surface atoms is often of the most interest.[17,18,20,21] This is not only due to the hydrogen bond lifetime and self-diffusion constant discussed above but also due to the biased orientation of water molecules near these surfaces. Figure 4 shows the water hydroxyl group orientation for both the $-CH_3$ and −COOH activated surfaces. The angle, θ, is defined as the angle between the surface normal and the nearest water O−H vector (closest H atom to the surface). Thus, for the O−H vector pointing right onto the surface, this angle is 180° with a cos(θ) value of −1.0. For the carboxyl surface, cos(θ) has a peak value of −0.6 to −0.7, which corresponds to a peak angle near 130°. This is not surprising given that water molecules are hydrogen bonded to the −COOH groups. The water OH groups are largely pointing to the carbonyl oxygen atom in the −COOH groups. The methyl surface also shows a negative peak for cos(θ) near −0.3 to −0.4, albeit a broader distribution. This corresponds to a broad angle distribution near 110°. The larger than 90° angle indicates that the first solvation shell water hydroxyl groups are largely pointing toward the hydrophobic surface. Thus, both graphite−CH_3 and graphite−COOH surfaces induce a large reorganization of water molecules. This is consistent with the previous findings that small scale hydrophobic solutes hydrate differently than large ones. Small solutes such as an argon atom or a methane molecule can fit into the water hydrogen bond network without destroying much of the hydrogen bonds,[14] whereas larger hydrophobic solutes such as the graphite−CH_3 plate induce reorganization of water such that hydroxyl groups point into the surface, thus producing dangling hydrogen bonds.[16]

3.2. Water Dynamics inside Double Plates. Now, we consider the water dynamics between the double plates. Both

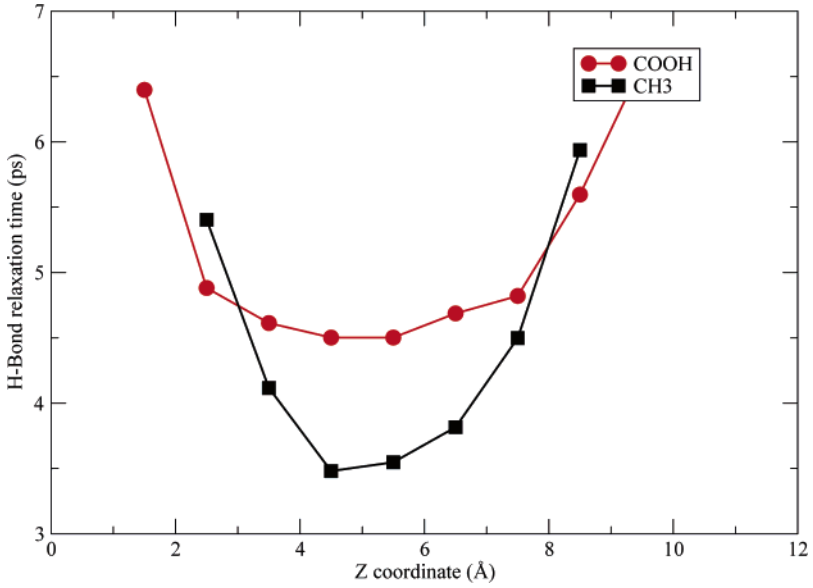

Figure 5. Water hydrogen bond relaxation time, τ, at various positions inside the interplate region for both methyl (black) and carboxyl (red) plates. A water layer of 3 Å thick parallel to the surface is again used for data averaging.

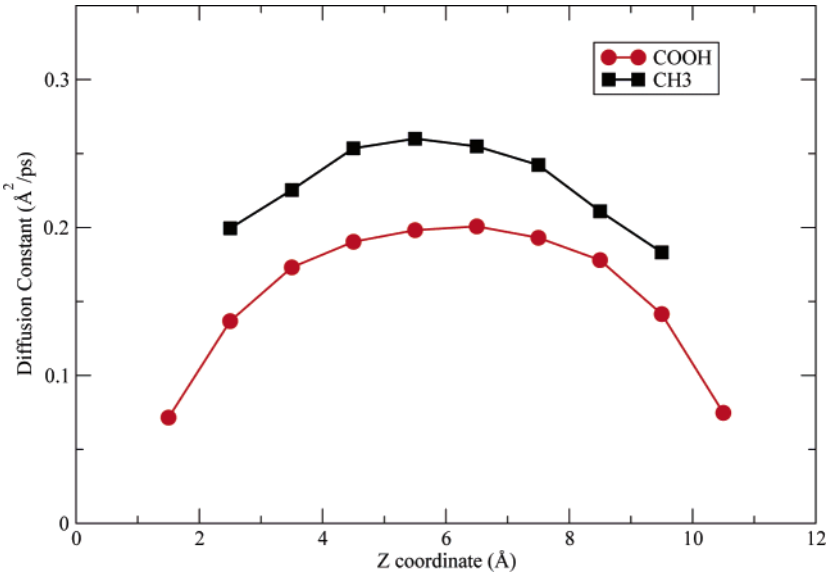

Figure 6. Water self-diffusion constant, D_w, at various positions inside the interplate region for both methyl (black) and carboxyl (red) plates. A water layer of 3 Å thick parallel to the surface is again used for data averaging.

methyl and carboxyl plates are studied with various plate−plate distances, D (D defined as the closest distance between the opposite active groups on both plates). From the discussion above, we know both surfaces can have significant influences on the behavior of water molecules. It is of great interest to see what kind of enhancement double plates can play on the water dynamics and what other effects the double plates can have, such as a possible water drying transition.

Figures 5 and 6 show the hydrogen bond lifetime and diffusion constant for water inside the double plates at $D = 13$ Å, respectively. The curves for the methyl plates have two fewer data points near the two opposite surfaces than do the carboxyl plates. This occurs since there are not enough water molecules to be collected near the methyl surfaces, which results from the partial water depletion near the hydrophobic surfaces (more discussions below). Again, we see much longer relaxation times and much smaller diffusion constants near the two surfaces as compared to the interdomain center region and the bulk water. The impact from the carboxyl surfaces is again more profound than the methyl surfaces. These results are consistent with the above results for the single plates. More interestingly, the double plates seem to have enhanced the surface influence on the water dynamics inside the interplate region. For example, the hydrogen bond lifetime near the center of the carboxyl double plates is about 4.50 ps, which is much larger than the single plate's 3.44 ps at the equivalent distance of 6 Å, and it is also much larger than the bulk value of 2.98 ps. The diffusion constant, on the other hand, is 0.20 Å^2/ps, which is smaller than 0.32 Å^2/ps in the single plate case and 0.375 Å^2/ps in the bulk. Similar behavior can be found for the methyl double plates as well. Thus, the effect of methyl and carboxyl groups on neighboring water dynamics is greatly enhanced by the double plates as compared to the single plates.

The next interesting question is then the following: Is there a dewetting transition in the methyl double plates when the plate−plate distance decreases to some threshold value? In general, there is no expectation to observe such a drying transition between the carboxyl plates, since there are strong electrostatic and van der Waals interactions between the −COOH groups and water molecules. It is known from previous

simulations[13,51,52] as well as macroscopic theory based on Young's equation that the critical distance for drying between the plates will decrease as the strength of the attractive interaction is increased.[51] For example, no dewetting is found between two very hydrophobic domain interfaces for a multidomain protein BphC enzyme, but dewetting occurs when the attractive electrostatic and van der Waals interactions between the protein and water are turned off.[13] On the other hand, a weak dewetting transition with a critical distance of about 7 Å is found for paraffin-like plates[52] and also a strong dewetting transition with a critical distance of 14 Å is observed for purely repulsive idealized plates with comparable sizes.[51] In general, it can be shown that, when the water contact angle, θ_c, for water in contact with the plate is obtuse, $D_c \propto \cos \theta_c$.[51] Since the contact angle decreases as the strength of the attraction between water and the plate increases, D_c should also decrease. For sufficiently strong attraction, one can expect θ_c to eventually become acute, at which point no drying transition will occur. In fact, for obtuse contact angles close to 90°, drying may be possible in principle, but not in practice, because the predicted D_c value gets so small that steric effects will not allow even a single layer of water to fit between the plates. Drying is thus very sensitive to the strength of the attractive forces. For example, at room temperature, the contact angle of water on graphite is known to be 86° from experiment (the simulated contact angle, on the other hand, depends on the water−carbon binding energy,[53] and it can be slightly larger than 90°) so that, if macroscopic theory is valid down to such small separations, drying should not occur.[54] What is the situation then for the current graphite−CH_3 plates? The sparse methyl groups on the graphite surface should presumably make the surface more hydrophobic; however, is it enough for a dewetting transition?

A series of 300 ps NPT simulations were performed for graphite−CH_3 double plates with the interplate distance, *D*, at 6.6, 7.0, 8.0, 9.0, and 10.0 Å, starting from the initial wet configurations (water molecules filling up the space initially). The last 100 ps data were used for the water density profile calculation, which is represented as the relative density along the *z*-axis, $\rho(z)/\rho_0$, with ρ_0 being the bulk density. Figure 7 shows the water density profile at some representative plate−plate distances. At the shortest separation, $D = 6.6$ Å (smallest distance to hold one layer of water sterically), a sharp peak appears in the density profile at the middle of the two plates, indicating a well-defined water monolayer at this separation. The trajectory movie also shows a clear monolayer of water molecules with a roughly planar hydrogen bond network. The average hydrogen bond number is found to be only 2.3 as compared with the bulk number 3.5. The strong density peaks just outside the two plates also indicate a strong layering of water molecules adjacent to the outside graphite surface of the hydrophobic plates. As the distance, *D*, increases to 10 Å, two well-defined peaks in the density profile appear between the two plates corresponding to two distinct layers of water molecules. This indicates that two intervening water layers can be held at this separation. The case of a separation of $D = 8$ Å falls between the above two cases, with one to two layers of water molecules inside the interplate region, which can be seen from the two small peaks in the water density profile. These results indicate that with the normal OPLSAA force field parameters the graphite−CH_3 plates do not exhibit a water dewetting transition. The presence of a monolayer of water at the smallest separation, $D = 6.6$ Å, persists even after continuing the simulation for over a nanosecond, indicating that the wet

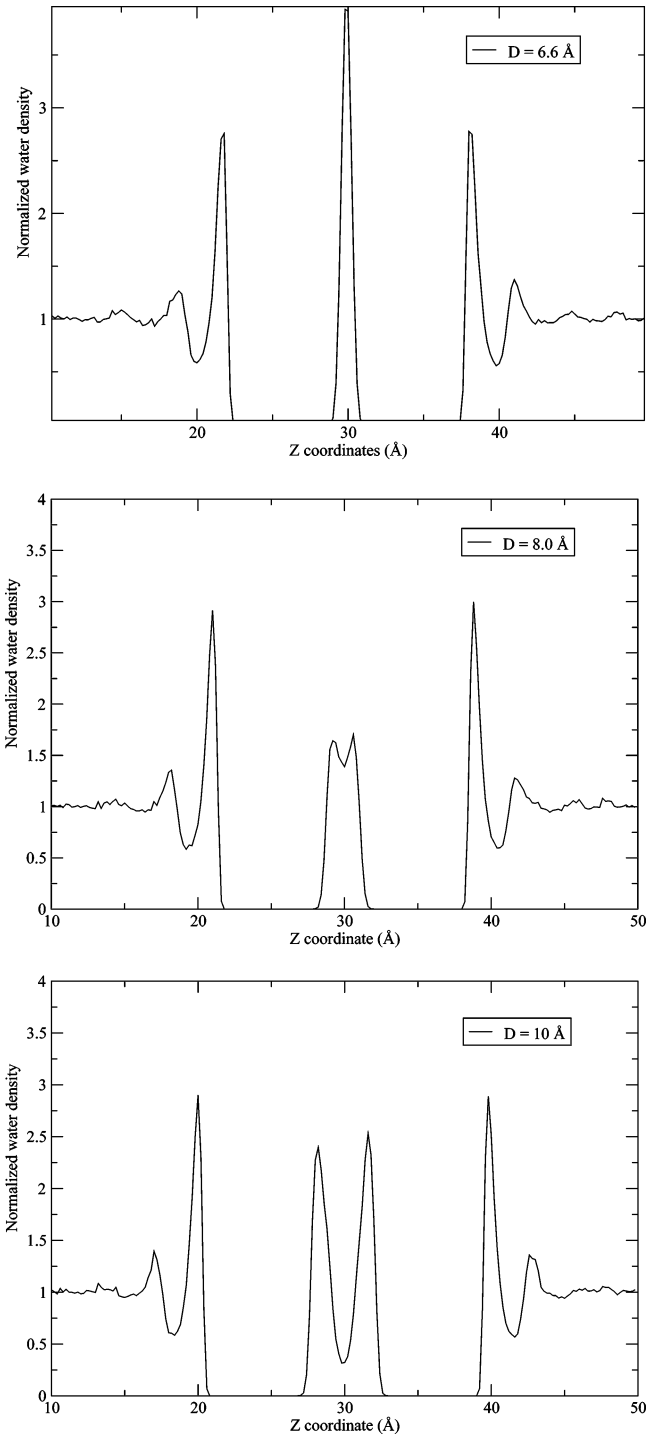

Figure 7. Normalized water density, $\rho(z)/\rho_0$ (ρ_0 is the bulk water density 1.0 g/cm^3), along the *z*-axis for the double graphite−CH_3 plates at various plate−plate distances, *D*, using normal OPLSAA force field parameters for the methyl groups. No dewetting is observed even at the smallest distance, $D = 6.6$ Å, which can hold one layer of water sterically.

configuration is thermodynamically more stable than the dry configuration.

To investigate how sensitive the dewetting phenomenon is related to the strength of the solute−solvent attractions, we also perform a series of similar simulations with reduced water−methyl interactions. We first turned off the charges on the −CH_3 groups by setting them to zero. No dewetting transition was observed, either. Similar water density profiles were found for all separations with somewhat reduced peak heights at smaller separations, but even at the smallest separation, $D = 6.6$ Å, a

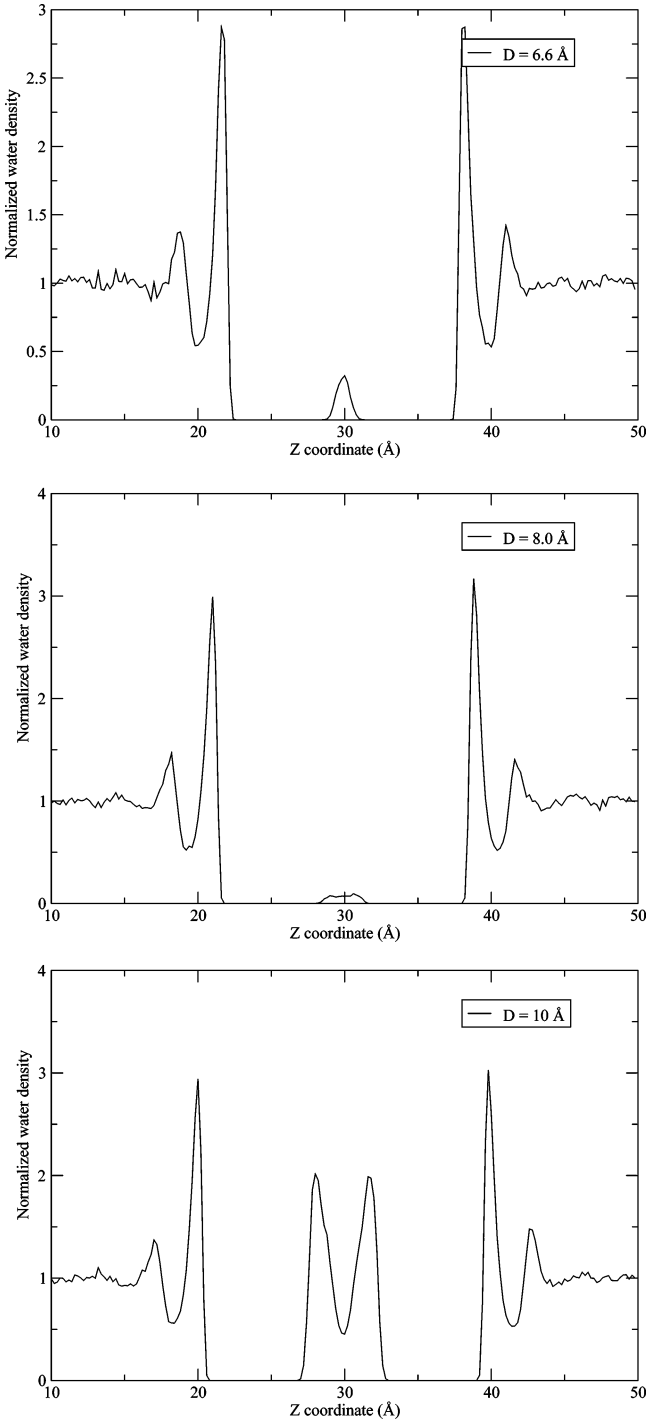

Figure 8. Normalized water density, $\rho(z)/\rho_0$, along the *z*-axis for the double graphite−CH_3 plates at various plate−plate distances, *D*, using reduced force field parameters for the methyl groups. Partial charges on the methyl C and H atoms are set to zero, and their van der Waals potential well depths, ϵ's, are reduced to a quarter of the original values. Dewetting transition has then been observed at distances of $D = 6.6$ Å and $D = 8.0$ Å. Detailed analysis shows that a critical distance, D_c, of 8−9 Å exists for this interaction-reduced system.

clear monolayer of water at the middle of the two plates persisted. We then further reduced the water−methyl van der Waals interactions by decreasing the ϵ's of the C and H atoms of the methyl group. Figure 8 shows the water density profiles at the same representative plate−plate distances, $D = 6.6$, 8.0, and 10.0 Å, when the C and H ϵ's have been reduced to 0.0165 and 0.0075 kcal/mol, which are about one-quarter of the original values. Interestingly, both the $D = 6.6$ Å and $D = 8.0$ Å cases show a sharp dewetting transition with essentially no water molecules inside the interplate region. The small nonzero density peaks between the plates are due to the way the water molecules are counted here; these are the water molecules near the edges of the plates, since we used the plate *xy* lateral sizes to define the interplate region. If we reduce the *xy* lateral sizes to be closer to the center, the density will be effectively zero. Trajectory movies confirmed these findings. After about 100 ps of NPT simulation, most of the water molecules were expelled from the center of the interplate region. However, the $D = 10$ Å case still shows two well-defined peaks in the interplate region, with only the peak heights slightly more reduced than those in Figure 7 from the normal potentials. The slightly lower peak heights are due to the fact that the "methyl" groups with reduced interactions are more hydrophobic; thus, a stronger water depletion effect is expected near each plate. These results indicate that, at this strength of water−solute interaction, a drying transition does occur, at a critical distance of about 8−9 Å. In other words, the hydrophobic surfaces can expel one to two layers of water molecules in order to get a a thermodynamically more stable dry state.

From the foregoing simulations, a simple picture emerges. Drying transitions do not occur between the graphite−CH_3 plates under the normal force field potential. Only when the water−methyl attractive interactions are reduced (no charges, and C/H van der Waals well depth reduced to one-quarter of the initial values, for example), the dewetting transition is observed with a critical distance of 8−9 Å under the current plate size, which can hold one to two layers of water molecules. It is interesting to note that, in recent computational studies by Hummer and co-workers of water inside a carbon nanotube and by Pettitt and co-workers[15,55] of water between two graphite plates, dewetting was not observed, either. Our results are consistent with these previous findings. On the other hand, Berne and co-workers[52] found that a weak dewetting exists in paraffin plates with a critical distance of about 7 Å (expelling one layer of water). It was pointed out that the solute−solvent attraction is approximately 2 times weaker in paraffin-like plates than in graphite plates.[52] Even though an exact comparison of the strength of the solute−solvent interaction for the current sparsely planted graphite−CH_3 plate and pure graphite plate is nontrivial, a reasonable estimate can be made on the basis of the equivalent Gay−Berne potential well depth.[51] The equivalent Gay−Berne potential well depth of the graphite−CH_3 plate is calculated to be −0.8 to −1.5 kcal/mol, depending on various locations on the graphite−CH_3 surface. This indicates that the graphite−CH_3 plate is more hydrophobic than the pure graphite plate (an equivalent Gay−Berne potential well depth of −1.83 kcal/mol[52]) but probably less hydrophobic than the paraffin plate (an equivalent Gay−Berne potential well depth of −0.91 kcal/mol[52]). The reason we use the equivalent Gay−Berne potential well depth for comparison is because we cannot simply compare the van der Waals ϵ alone due to the different compactness of C atoms in graphite, graphite−CH_3, and paraffin molecules. Thus, the current graphite−CH_3 plate falls between the pure graphite plate and the paraffin plate in terms of the hydrophobicity. As mentioned earlier, a simple macroscopic thermodynamic model based on Young's equation allows one to approximately predict the critical distance for drying.[51] This critical distance depends on the size of the plates and the contact angle between the plate and water. For a given plate size, the larger the contact angle, the greater will be the critical distance. On the other hand, the larger the attractive interaction between the plates and water, the smaller will be the contact angle.

Interestingly, Lundgren et al.[54] have recently studied the water contact angle versus the Lennard-Jones potential well depth, ϵ, between the solute and solvent using a graphite-like geometry. On the basis of their calculation,[54] the contact angle for paraffin is estimated to be about 115°,[52] which gives a critical distance of 7−9 Å according to the macroscopic theory (Figure 6 in ref 52). This is in excellent agreement with our computer simulation for paraffin plates.[52] The current graphite−CH_3 plates are then estimated to have a contact angle between 86° (pure graphite) and 115° (paraffin) on the basis of the above hydrophobicity strength analysis. Even if we assume the contact angle to be about 100°, the critical distance for the double graphite−CH_3 plates (with comparable sizes to those of the previous paraffin plates[52]) will be approximately 3−4 Å from the macroscopic theory (see Figure 6 of ref 52), which clearly cannot hold one layer of water molecules sterically. The graphite−CH_3 plates must be approximately 6.6 Å apart to accommodate one layer of water. Thus, no dewetting transition should be expected for graphite−CH_3 plates, as confirmed by our computer simulation. For the plates with reduced interactions, however, the water contact angle will increase to above 115° and dewetting should be expected for this size of plates. Our computer simulation result with a critical distance, D_c, of 8−9 Å also agrees very well with the prediction from macroscopic theory.[52] Finally, it is interesting to point out that, for purely repulsive hydrophobic plates, the contact angle will be approaching 180° and the critical distance will be even greater for plates with similar sizes, as seen in the previous studies on the idealized hydrophobic plates,[51] a two-domain protein with no attractive protein−water interactions,[13] and graphite plates with purely repulsive interactions.[55]

4. Conclusion

In this study, we have performed molecular dynamics simulations of a newly designed system composed of methyl/carboxyl planted graphite sheets to mimic the interaction between hydrophobic/hydrophilic groups and solvent water molecules. Our results indicate that the model system can clearly demonstrate the interesting surface effects on water dynamics, such as the breaking of water hydrogen bonding networks and attenuating solvent mobility. The hydrogen bond lifetime near hydrophobic and hydrophilic surfaces can be increased by a factor of 2, and the diffusion constant can be diminished on the other hand by as much as a factor of 8. The hydrophilic carboxyl surfaces are found to have an even more profound influence on the water dynamics than do the hydrophobic methyl surfaces. The water orientation near the first solvation shell of the hydrophilic carboxyl groups shows a sharp peak in the angle between the nearest hydroxyl group and surface normal, indicating a strong bias in hydroxyl group orientation in order to make hydrogen bonds with the carboxyl groups. The methyl groups also show a clear bias but with a somewhat broader distribution in the water orientation by pointing the hydroxyl group toward the hydrophobic surface. The model systems also reveal interesting behavior about the water dynamics inside the double plates as well as the possible dewetting transition between the hydrophobic graphite−CH_3 plates. No dewetting transition was found for the graphite−CH_3 plates with normal force field potentials, but with the water−methyl attractive interactions reduced (no charges and C/H van der Waals potential well depth reduced to one-quarter of the original values), a sharp dewetting transition was observed with a critical distance of 8−9 Å which can hold one to two layers of water molecules. Furthermore, the relationship among the dewetting transition critical distance, van der Waals potential well depth, and water contact angle on the solute surface is analyzed in detail on the basis of a simple macroscopic theory, which can be used to predict the dewetting transition critical distance. These investigations have important implications for the hydrophobic interaction mechanism behind self-assembly processes of many biosystems, such as protein folding, lipid formation, and micelle formation.

Future work will be conducted along the lines toward more realistic but still amenable systems to enable a more direct comparison with biological systems. One such example is to invoke a mixed methyl and carboxyl group plate with different percentages of composition to mimic the protein hydrophobic core and hydrophilic exterior. This arrangement might help us to decode the complicated interactions involved when a mixed environment is present. For example, others have observed the following ranking relationship for water hydrogen bond lifetime and water residence time near various residues in a protein: $\tau_{charged} > \tau_{polar} > \tau_{nonpolar}$, for many proteins such as crambin,[56] plastocyanin,[57] and azurin.[58] However, for bovine pancreatic trypsin inhibitor (BPTI), such a relationship among nonpolar, polar, and charged residues was not observed.[59,60] Clearly, the complex interactions of water with various neighboring residues complicate the situation and blur distinguishing between nonpolar, polar, and charged residues. A well designed system with mixed methyl and carboxyl groups might shed light on this important problem.

Acknowledgment. We would like to thank Xuhui Huang for the help of the equivalent Gay−Berne potential well depth calculation for the graphite−CH_3 plates and Bruce Berne, Jed Pitera, Gerhard Hummer, David Silverman, and Zhijian Wang for many helpful discussions and comments.

References and Notes

(1) Brooks, C. L.; Onuchic, J. N.; Wales, D. J. *Science* **2001**, *293*, 612.
(2) Dobson, C. M.; Sali, A.; Karplus, M. *Angew. Chem., Int. Ed. Engl.* **1998**, *37*, 868.
(3) Brooks, C. L.; Gruebele, M.; Onuchic, J. N.; Wolynes, P. G. *Proc. Natl. Acad. Sci. U.S.A.* **1998**, *95*, 11037.
(4) Zhou, Y.; Karplus, M. *Nature* **1999**, *401*, 400.
(5) Hummer, G.; Garde, S.; Garcia, A. E.; Pratt, L. R. *Chem. Phys.* **2000**, *258*, 349.
(6) Beckstein, O.; Biggin, P. C.; Sansom, M. S. P. *J. Phys. Chem. B* **2001**, *105*, 12902.
(7) Beckstein, O.; Sansom, M. S. P. *Proc. Natl. Acad. Sci. U.S.A.* **2003**, *100*, 7063.
(8) Luzar, A.; Leung, K. *J. Chem. Phys.* **2000**, *113* (14), 5836.
(9) Leung, K.; Luzar, A.; Bratko, D. *Phys. Rev. Lett.* **2003**, *90*, 65502-1.
(10) Lum, K.; Luzar, A. *Phys. Rev. E.* **1997**, *56* (6), 6283.
(11) Cheng, Y.; Rossky, P. J. *Nature* **1998**, *392*, 696.
(12) Zhou, R. *Proc. Natl. Acad. Sci. U.S.A.* **2003**, *100*, 13280.
(13) Zhou, R.; Huang, X.; Margulius, C. J.; Berne, B. J. *Science* **2004**, *305*, 1605.
(14) Pangali, C.; Rao, M.; Berne, B. J. *J. Chem. Phys.* **1979**, *71*, 2975.
(15) Hummer, G.; Rasaiah, J. C.; Noworyta, J. P. *Nature* **2001**, *414*, 188.
(16) Lee, C. Y.; McCammon, J. A.; Rossky, P. J. *J. Chem. Phys.* **1984**, *80*, 4448.
(17) Xu, H.; Berne, B. J. *J. Phys. Chem. B* **2001**, *105*, 11929.
(18) Bizzarri, A. R.; Cannistraro, S. *J. Phys. Chem. B* **2002**, *106*, 6617.
(19) Tarek, M.; Tobias, D. J. *Biophys. J.* **2000**, *79*, 3244.
(20) Hayashi, T.; Pertsin, A. J.; Grunze, M. *J. Chem. Phys.* **2002**, *117*, 6271.
(21) Zangi, R. *J. Phys.: Condens. Matter* **2004**, *16*, S5371.
(22) Stillinger, F. H.; David, C. W. *J. Chem. Phys.* **1978**, *69*, 1473.
(23) Lum, K.; Chandler, D.; Weeks, J. D. *J. Phys. Chem. B* **1999**, *103*, 4570.
(24) Huang, D. M.; Chandler, D. *J. Phys. Chem. B* **2002**, *106*, 2047.
(25) Huang, D. M.; Chandler, D. *Proc. Natl. Acad. Sci. U.S.A.* **2000**, *97*, 8324.

(26) Wolde, P. R. T.; Sun, S. X.; Chandler, D. *Phys. Rev. E* **2001**, *65*, 011201.
(27) Wolde, P. R. T.; Chandler, D. *Proc. Natl. Acad. Sci. U.S.A.* **2002**, *99*, 6539.
(28) Wallqvist, A.; Berne, B. J. *J. Phys. Chem.* **1995**, *99*, 2885.
(29) Wallqvist, A.; Gallicchio, E.; Levy, R. M. *J. Phys. Chem. B* **2001**, *105*, 6745.
(30) Paulaitis, M. E.; Pratt, L. R. *Adv. Protein Chem.* **2002**, *62*, 283.
(31) Pratt, L. R. *Annu. Rev. Phys. Chem.* **2002**, *53*, 409.
(32) Talanquer, V.; Oxtoby, D. W. *J. Chem. Phys.* **1995**, *103*, 3686.
(33) Bratko, D.; Curtis, R. A.; Blanch, H. W.; Prausnitz, J. M. *J. Chem. Phys.* **2001**, *115*, 3873.
(34) Abhijit, V. Shedvade, S. J.; Gubbins, K. E. *J. Chem. Phys.* **2000**, *113*, 6933.
(35) Steitz, R.; Gutberlet, T.; Hauss, T.; Klosgen, B.; Krastev, R.; Schemmel, S.; Simonsen, A. C.; Findenegg, G. H. *Langmuir* **2003**, *19*, 2409.
(36) Jensen, T. R.; Jensen, M. O.; Reitzel, N.; Balashev, K.; Peters, G. H.; Kjaer, K.; Bjornholm, T. *Phys. Rev. Lett.* **2003**, *90(8)*, 86101-1.
(37) Jensen, M. O.; Mouritsen, O. G.; Peters, G. H. *J. Chem. Phys.* **2004**, *120*, 9729.
(38) Ball, P. *Nature* **2003**, *423*, 25.
(39) Lindahl, E.; Hess, B.; van der Spoel, D. *J. Mol. Model.* **2001**, *7*, 306.
(40) Jorgensen, W. L.; Maxwell, D.; Tirado-Rives, J. *J. Am. Chem. Soc.* **1996**, *118*, 11225.
(41) Allen, M. P.; Tildesley, D. J. *Computer Simulation of Liquids*; Oxford University Press: Oxford, U.K., 1987.
(42) Pal, S.; Balasubramanian, S.; Bagchi, B. *J. Chem. Phys.* **2004**, *120*, 1912.
(43) Starr, F. W.; Nielsen, J. K.; Stanley, H. E. *Phys. Rev. E* **2000**, *62*, 579.
(44) Kohlrausch, R. *Ann. Phys. (Leipzig)* **1847**, *12*, 353.
(45) Williams, G.; Watts, D. C. *Trans. Faraday Soc.* **1870**, *66*, 80.
(46) Pu, L.; Harder, E.; Berne, B. J. *J. Phys. Chem. B* **2004**, *108*, 6595.
(47) Balasubramanian, S.; Bandyopadhyay, S.; Pal, S.; Bagchi, B. *Curr. Sci.* **2003**, *85*, 1571.
(48) Risken, H. *The Fokker−Planck Equation*; Springer: Berlin, 1989.
(49) Dastidar, S. G.; Mukhopadhyay, C. *Phys. Rev. E* **2003**, *68*, 021921.
(50) Rocchi, C.; Bizzarri, A. R.; Cannistraro, S. *Phys. Rev. E* **1998**, *57*, 3315.
(51) Huang, X.; Margulis, C. J.; Berne, B. J. *Proc. Natl. Acad. Sci. U.S.A.* **2003**, *100*, 11953.
(52) Huang, X.; Zhou, R.; Berne, B. J. *J. Phys. Chem. B* **2005**, *109*, 3546.
(53) Werder, T.; Walther, J. H.; Jaffe, R.; Halicioglu, T.; Noca, F.; Koumoutsakos, P. *Nano Lett.* **2001**, *1*, 697.
(54) Lundgren, M.; Allen, N. L.; Cosgrove, T. *Langmuir* **2002**, *18*, 10462.
(55) Choudhury, N.; Pettitt, B. M. *J. Phys. Chem. B* **2005**, *109*, 6422−6429.
(56) Garcia, A. E.; Stiller, L. *J. Comput. Chem.* **1993**, *14*, 1396.
(57) Rocchi, C.; Bizzarri, A. R.; Cannistraro, S. *Chem. Phys.* **1997**, *214*, 261.
(58) Luise, A.; Falconi, M.; Desideri, A. *Proteins* **2000**, *39*, 56.
(59) Brunne, R. M.; Liepinsh, E.; Otting, G.; Wuthrich, K.; vanGunsteren, W. F. *J. Mol. Biol.* **1993**, *231*, 1040.
(60) Muegge, I.; Knapp, E. W. *J. Phys. Chem.* **1995**, *99*, 1371.